ISBN: 978-3-95450-223-3 ISSN: 2673-7000 doi:10.18429/JACoW-NAPAC2019-MOPLO18

THERMAL ANALYSIS OF THE LANSCE H+ RFQ TEST STAND FARADAY CUP*

E. N. Pulliam#, I. N. Draganic, J. L. Medina, J. P. Montross, J. F. O'Hara, L. J. Rybarcyk
Los Alamos National Laboratory, Los Alamos, NM, USA

Abstract

The Los Alamos Neutron Science Center (LANSCE) operates one of the nation's most powerful linear accelerators (LINAC). Currently the facility utilizes two 750 keV Cockcroft-Walton (CW) based injectors for transporting H+ and H- beams into the 800 MeV accelerator. A Radio Frequency Quadrupole (RFQ) design is being proposed to replace the aged CW injectors. An important component of the RFQ Test Stand is the Faraday cup that is assembled at the end of the Low Energy Beam Transport (Phase 1 LEBT) and Medium Energy Beam Transport (Phase 3 MEBT). The Faraday cup functions simultaneously as both a beam diagnostic and as a beam stop for each of the three project phases. This paper describes various aspects of the design and analysis of the Faraday cup. The first analysis examined the press fit assembly of the graphite cone and the copper cup components. A finite element analysis (FEA) evaluated the thermal expansion properties of the copper component, and the resulting material stress from the assembly. Second, the beam deposition and heat transfer capability were analyzed for LEBT and MEBT beam power levels. Details of the calculations and analysis will be presented.

INTRODUCTION

LANSCE functions as a National User Facility with the LINAC supporting fundamental research and science for a wide variety of projects including isotope production, materials research, proton radiography, and more. The facility was originally opened in 1972 and used a state of the art Cockcroft-Walton based injector system to transfer H^+ and H^- beams into the 800 MeV accelerator. These injector systems are difficult to maintain and operate, and currently an RFQ based design is being developed to replace them [1]. The RFQ design is intended to modernize the facility and reduce long term operational risks. An RFQ is a high current structure that simultaneously accelerates and focuses the charged particle beam. Integrating this system into the current LINAC has the potential to improve beam reliability and production. An RFQ Test Stand is being assembled at the LANSCE H^+ RFQ injector lab to test performance of the Kress-GmbH designed RFQ [2]. Figure 1 shows the current assembly of the Test Stand LEBT.

An important piece of the RFQ Test Stand is the Faraday cup that is located at the end of the Phase 1 LEBT and Phase 3 MEBT. The Faraday cup functions simultaneously as both a beam diagnostic and as a beam stop for each of the three phases [3]. Multiple analysis steps were required to validate that the design was appropriate for its intended use. This paper describes various aspects of the design, assembly, and analysis of the LANSCE RFQ Faraday cup.

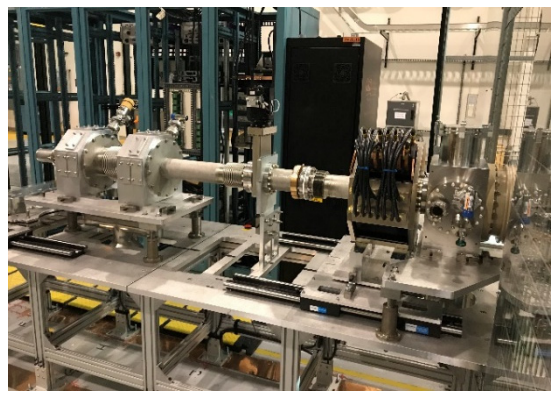

Figure 1: H^+ RFQ Test Stand LEBT assembly.

FARADAY CUP DESIGN

The unique Faraday cup design accomplishes multiple tasks for the RFQ Test Stand. The assembly acts as a beam stop for multiple phases of testing, a beam current measurement system, and serves as a mechanism for heat dissipation. Figure 2 shows the individual components, assembly, and internal section view of the Faraday cup.

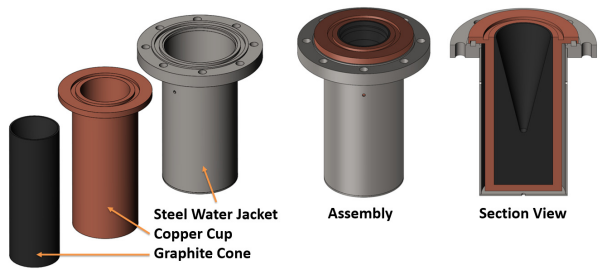

Figure 2: H^+ RFQ Test Stand Faraday cup components.

The beam direction is perpendicular to the top face and is deposited into the graphite cone. The conical section of the graphite is designed so the beam has a large surface area to deposit into, and helps reduce secondary electrons. The graphite is captured inside the copper using a tight interference fit to improve heat transfer. Electrical connections are made to the copper flange allowing for beam current measurement. The copper cup is surrounded by the flanged stainless steel jacket which has an internal water channel that directly cools the outer copper surfaces. This stainless steel flange is then bolted to the end of the beamline. The assembly also uses a pair of MACOR® [4] ring insulators on either side of the copper cup flange in order to isolate

* Work supported by the United States Department of Energy, National Nuclear Security Agency, under contract DE-AC52-06NA25396
# eliasp@lanl.gov

ISBN: 978-3-95450-223-3 ISSN: 2673-7000 doi:10.18429/JACoW-NAPAC2019-MOPLO18

the graphite and copper from the steel jacket. The uniqueness of this assembly required multiple analyses to verify its proper operation.

THERMAL EXPANSION ANALYSIS

The first analysis examined the press fit assembly of the graphite cone and the copper cup components. Expansion of the copper cup during heating was analyzed to confirm that the design constraints allowed the graphite cone to mate properly in the copper cup. The design had an interface overlap of nearly 3 thousandths of an inch so the copper needed to expand by slightly more to accept the graphite. An FEA of the thermal expansion was set up with a 150 °C heat load on the copper outer cylindrical surfaces and base to model the heating. The entire model was given a conservative free air convection coefficient of 5 W/m^{2}K. This resulted in uniform heating of the copper cup and the thermal contour plot can be seen in Fig. 3.

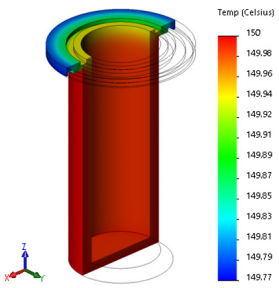

Figure 3: Thermal profile of the copper cup after heat loads were applied.

This thermal profile was then imported as a thermal load into a static displacement analysis to evaluate the resulting thermal expansion. The model was allowed to freely expand due to the heating. This resulted in the radial displacement contour plot seen in Fig. 4. The resulting displacement of the copper cup due to thermal expansion was adequate for allowing the graphite to fit.

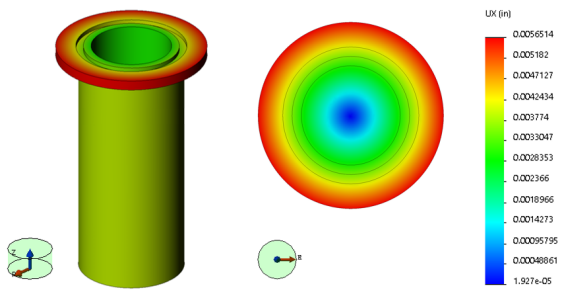

Figure 4: Thermal expansion radial displacement plots.

INTERFERENCE FIT ANALYSIS

An analysis was done to ensure the interference fit assembly process would not result in excessive stress in the copper cup or the graphite cone. The FEA evaluated the average stress, contact pressure, and tangential stress (hoop stress). Two conditions were assessed for the interference fit calculations: One was the thinnest section of the graphite cone and the other was the solid graphite section. Solidworks Simulation was used to perform the FEA with a shrink fit contact and interface overlap of 3 thousandths of an inch. Figures 5 and 6 show the contour plots for the average stress and hoop stress resulting from the assembly.

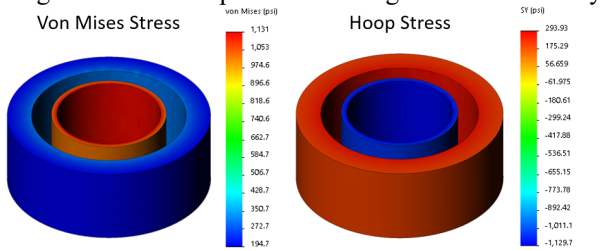

Figure 5: Deformed stress plots for thinnest graphite.

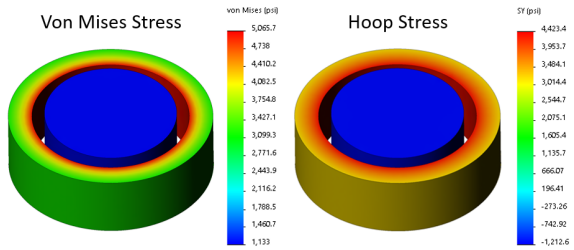

Figure 6: Deformed stress plots for solid graphite.

The analysis was compared with calculations to check validity of the FEA. Equation 1 was used to determine the contact pressure (p) based on material properties and geometrical constraints. The radial interface (δ) of the graphite and copper was 0.0015 inches. The subscripts are for the inner member (i) and outer member (0) respectively. The external radius (R) and internal radius (r) were defined by the design constraints for each geometrical condition. Poisson's ratio (v) and elastic modulus (E) for each material were used. Equations 2 and 3 were used to calculate the hoop stress (σ_t) at the transition radius for the internal and external member respectively. When evaluating the FEA results and the calculated values they were very close and it gave confidence that the FEA was valid. Material yield limits were not met in any cases so the interference fit assembly was confirmed to be safe.

$$p = \frac{\delta}{\left[\frac{1}{E_0}\left(\frac{r_0^2 + R^2}{r_0^2 - R^2} + v_0\right) + \frac{1}{E_i}\left(\frac{R^2 + r_i^2}{R^2 - r_i^2} - v_i\right)\right]} \quad (1)$$

$$\sigma_{t_i} = -p\left(\frac{R^2 + r_i^2}{R^2 - r_i^2}\right) \quad (2)$$

$$\sigma_{t_o} = p\left(\frac{r_0^2 + R^2}{r_0^2 - R^2}\right) \quad (3)$$

BEAM POWER DISTRIBUTION

Beam power in the LEBT and MEBT is modeled as a Gaussian distribution with the beam diameter as estimated in [5], with the H^+ beam radius near 2.3 cm (0.9 in). The total beam power was calculated in Table 1 using the projected values for the RFQ Test Stand. This total power was

ISBN: 978-3-95450-223-3 ISSN: 2673-7000 doi:10.18429/JACoW-NAPAC2019-MOPLO18

distributed between different split surfaces on the graphite cone that represented the total beam diameter.

Table 1: Beam Characteristics for the LEBT and MEBT

Test Stand Phase	Energy (keV)	Duty Factor (%)	Average Current (mA)	Beam Power (W)
LEBT	35	15	7.5	263
MEBT	750	7.5	1.58	1180

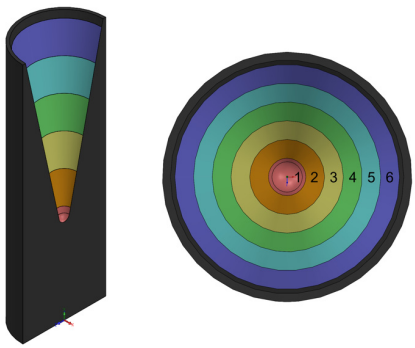

Figure 7: Split surfaces on graphite cone showing an internal section and top view respectively.

Figure 7 shows these different split surfaces with increments of 0.3 inches radially. The distribution is axially symmetric and was used to determine diameters of the split surfaces on the graphite cone and calculate heat flux on each surface. Table 2 shows the Gaussian percentage of the total beam power, the surface area of each split section, and the heat flux for that area. Total beam power for the LEBT was conservatively estimated as 300 W, and the calculated value in Table 1 (1180 W) was used for the MEBT.

Table 2: LEBT & MEBT Heat Flux Values

Section	Percent of Total Power	Surface Area (mm^2)	LEBT Heat Flux (kW/m^2)	MEBT Heat Flux (kW/m^2)
1	38.2	122.6	935.0	3677.5
2	30.0	632.3	142.5	560.0
3	18.4	1051.6	52.5	206.5
4	8.8	1477.4	18.0	70.0
5	3.4	1896.8	5.4	21.1
6	1.2	2316.1	1.6	6.1

HEAT TRANSFER COEFFICIENT

The steel water jacket was best represented as a concentric tube annulus for calculating the proper heat transfer coefficient for the analysis. The cooling liquid is near room temperature water flowing at 1 gpm, which provides an adequate temperature drop. The following calculations show the details of how the heat transfer coefficient was determined for the subsequent FEA. The hydraulic diameter (D_h) was 6.2 mm. The volumetric flow rate (Q) for water at 1 gpm and 20 °C is 63100 mm3/s, and has a kinematic viscosity (ν) of 1.004 mm2/s. The cross sectional area (A) was 682 mm2. Using these values in equation 4, the Reynold's number (Re) is calculated as 571.35.

$$\mathrm{R_e} = \frac{QD_h}{\nu A} \tag{4}$$

$$h = \left(\frac{48}{11}\right)\left(\frac{k}{D_h}\right) \tag{5}$$

Therefore the flow is characterized as fully laminar in the water jacket because Re is below 2300 [6]. Thus equation 5 applies for calculating the proper heat transfer convection coefficient [7]. Taking the thermal conductivity of water as 0.606 W/m2K the heat transfer coefficient is calculated as 426.5 W/m2K.

HEAT TRANSFER ANALYSIS

The heat transfer FEA used beam power levels for the LEBT and MEBT test phases as the heat load, and the calculated heat transfer coefficient as convective cooling. Results found that the Faraday cup would not exceed temperatures beyond material limits and would successfully operate. The thermal contour plot with individual color bars for the LEBT and MEBT load case results are shown in Fig. 8.

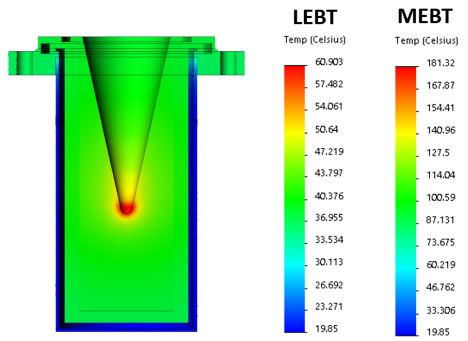

Figure 8: Thermal contour plot with temperature values for LEBT and MEBT respectively.

SUMMARY

The analysis of the Faraday cup determined that the component would operate acceptably for each phase of the RFQ Test Stand, and will be integrated into the production assembly in the future (Fig. 9). This unique accelerator component design highlights the multifunctional potential of the Faraday cup and the analysis steps needed to ensure its proper operation prior to installation.

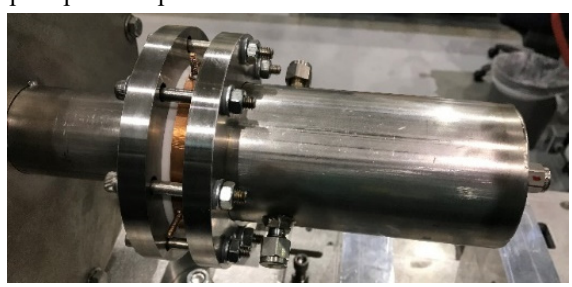

Figure 9: Faraday cup assembled at the LEBT end.

ISBN: 978-3-95450-223-3 ISSN: 2673-7000 doi:10.18429/JACoW-NAPAC2019-MOPLO18

REFERENCES

[1] R. W. Garnett *et al.*, "LANSCE H+ RFQ Status", in *Proc. IPAC'15*, Richmond, VA, USA, May 2015, pp. 4073-4075. doi:10.18429/JACoW-IPAC2015-THPF148

[2] L. Rybarcyk *et al.*, "Design Requirements and Expected Performance of the New LANSCE H+ RFQ", in *Proc. NA-PAC'13*, Pasadena, CA, USA, Sep.-Oct. 2013, paper MOPMA17, pp. 336-338.

[3] R. C. McCrady, *et al.*, "Diagnostics for the LANSCE RFQ Front-End Test Stand", in *Proc. NAPAC'13*, Pasadena, CA, USA, Sep.-Oct. 2013, paper MOPSM05, pp. 354-356.

[4] Corning, https://www.corning.com/worldwide/en/products/advanced-optics/product-materials/specialty-glass-and-glass-ceramics/glass-ceramics/macor.html

[5] Y. K. Batygin, *et al.*, "Design of low energy beam transport for new LANSCE H^+ injector." *Nuclear Instruments and Methods in Physics Research Section A: Accelerators, Spectrometers, Detectors and Associated Equipment*, vol. 753, pp. 1-8 (2014).

[6] F. P. Incropera, *et al.*, *Fundamentals of heat and mass transfer*. USA: Wiley, 2007.

[7] F. Kreith, R. M. Manglik, and M. S. Bohn, *Principles of heat transfer*. Stamford, CT, USA: Cengage Learning, 2012.